Revolutionizing Diagnostic Insights: Exploring Advanced Image Processing Techniques and Neural Networks in Traditional Indian Medicine

R. Srinivasan
College of Engineering and Design, Alliance University, Banglaore, India
rsrinivasanPHD720@ced.alliance.edu.in (corresponding author)

Reeba Korah
College of Engineering and Design, Alliance University, Banglaore, India
reeba.korah@alliance.edu.in

M. Ravichandran
Government Siddha College (Arumbakkam), The Tamilnadu MGR Medical University, Chennai, India
sreeveeka.rv@gmail.com

Received: 11 September 2024 | Revised: 12 October 2024, 26 October 2024, and 2 November 2024| Accepted: 19 November 2024

 DOI: https://doi.org/10.48084/etasr.8975

ABSTRACT

The Siddha and Ayurveda traditional Indian medicine practices utilize non-invasive diagnostic methods, such as Neikuri and Taila Bindu Pariksha, for patient diagnosis through urine analysis. While these methods have proven effective for centuries, their accuracy highly depends on the subjective experience of practitioners. To address this limitation, this study explores the use of advanced image processing techniques and deep learning, specifically Convolutional Neural Networks (CNNs), to automate and enhance diagnostic image analysis. This study utilized five pre-trained CNN models, namely DenseNet, ResNet, VGG-19, Inception, and EfficientNet, on a dataset of Neikuri images acquired from a Siddha medical institute, to standardize and improve the accuracy of patient diagnosis. The comparative evaluation revealed DenseNet as the best-performing model, achieving a classification accuracy of 93.33%, while Inception v3 followed with 90.5%. This study highlights the potential of integrating modern neural networks with traditional diagnostic practices, paving the way for more objective, efficient, and accessible healthcare solutions in traditional Indian medicine.

Keywords-Convolutional Neural Networks (CNNs); deep learning; traditional medicine; Siddha; Ayurveda; urine test images; patient diagnosis; medical image analysis; Neikuri; Taila Bindu Pariksha; Mutra Pariksha

I. INTRODUCTION

Traditional medical methods such as Siddha and Ayurveda employ established noninvasive urine diagnostic practices, such as Neikuri and Taila Bindu Pariksha [1, 2]. While these methods have proven valuable, particularly during the COVID-19 pandemic, their accuracy often depends on the experience of the practitioners [3]. The lack of standardized image datasets for training makes it challenging to ensure consistent diagnostic proficiency. This study investigates the use of Convolutional Neural Networks (CNNs), a state-of-the-art deep learning approach, to enhance these traditional practices. By incorporating CNNs, the aim is to enhance the precision, efficiency, and objectivity of these diagnostic methods, facilitating the training of novice practitioners and potentially leading to improved healthcare outcomes.

II. BACKGROUND AND METHODOLOGY

This study focuses on the application of CNNs to analyze diagnostic images derived from oil droplet observation techniques used in Neikuri and Taila Bindu Pariksha. These methods, while traditional, provide unique visual patterns that are challenging to classify using conventional image analysis methods. The goal of this research is to leverage deep learning models, specifically CNNs, to standardize and improve the classification of these images. A major challenge in this endeavor is the lack of standardized image datasets, which limits the ability to train machine learning models for accurate, reproducible analysis. This study addresses this challenge by developing a dataset of categorized images and evaluating various CNN architectures to identify the most effective model for this type of image classification.

A. Foundations of Siddha and Ayurveda Prognosis

Siddha medicine employs Naadi Parisodhana, a pulse diagnosis technique involving the radial artery at 27 points. This method assesses the dasa naadis (energy channels) and three humors (mukkutram) through variations in pulse strength, rhythm, and subtle qualities. These variations are believed to indicate imbalances and predict disease progression. Additionally, Neerkuri analysis of urine colour, taste, and sediment offers insight into digestive, metabolic, and kidney function, aiding in prognosis [4-7]. Ayurveda also utilizes Naadi Pariksha, with pulse qualities playing a key diagnostic role. Mutra Pariksha, the examination of urine colour, consistency, and other characteristics, contributes significantly to health assessments. Furthermore, Jivha Pariksha (tongue examination), Mala Pariksha (stool assessment), and Shabda Pariksha (voice examination) contribute to a comprehensive diagnostic framework. These traditional practices emphasize a holistic approach, combining various methods to provide a nuanced understanding of individual health, focusing on both prevention and treatment [8-11].

Although Neikuri and Taila Bindu Pariksha have historical significance, this study focuses purely on the technical aspects of analyzing the images they produce. These diagnostic images display patterns that can be complex, with subtle variations in shape, color, and dispersion. The ambiguity of these visual patterns makes them ideal candidates for deep learning techniques that can detect intricate features not easily discernible by the human eye. This study focuses on using CNNs to classify these images, regardless of the traditional medical practices from which they originate.

B. Image Acquisition from Siddha Institute

To acquire a comprehensive dataset for the Neikuri process in Siddha medicine, permission was obtained from the Government College of Siddha in Arumbakkam, Chennai, India. The dataset includes images representing various health conditions and their respective prognoses. To enhance the dataset's diversity, each image underwent careful preprocessing to preserve distinctive characteristics while being converted to grayscale and optimized for size. Given the initial dataset's limitations, an augmentation technique was implemented by rotating the images in increments of 10° up to a full 360° rotation. Then, each rotated image was saved as a distinct entry, effectively expanding the dataset. Subsequently, a Python code randomly divided the augmented dataset into training and test sets, maintaining a 70:30 ratio. This meticulous process ensures that the machine learning models are trained on a diverse range of images, enhancing their ability to accurately classify and diagnose different health conditions in alignment with the Neikuri process within the Siddha System.

C. Inference

Using CNNs to analyze Neikuri and Taila Bindu Pariksha images helps improve diagnostic accuracy by detecting subtle patterns that are hard to spot manually. By creating a diverse dataset and applying deep learning, this method can better classify health conditions and offer a modern, reliable approach to traditional diagnostic practices. This research bridges traditional medicine with advanced technology, making diagnoses more consistent and effective.

III. DEEP LEARNING ON THE NEIKURI IMAGES

Leveraging pre-trained CNN models is a well-established approach for accelerating the development process. This study employed five pre-trained CNN architectures, each meticulously chosen after a thorough examination of their design and operational principles. To ensure consistency, a standardized evaluation process was applied to each pre-trained model.

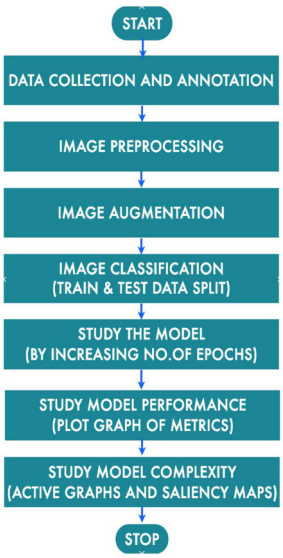

Fig. 1. The process flow of this research.

A. Selecting the Right Algorithm for the Neikuri images

The inherent ambiguity of the Neikuri images, characterized by their lack of well-defined shapes, low contrast, and subtle color variations, poses significant challenges for traditional machine learning models [12-16]. These images often display indistinct oil droplet dispersions, where subtle variations in texture and tonal shifts are critical for diagnostic interpretation. To address this challenge and achieve optimal performance, a comparative analysis of five pre-trained CNN models, namely DenseNet, ResNet, VGG-19, Inception, and EfficientNet, was carried out, focusing on their architectural strengths and weaknesses for handling these unique medical images. CNNs excel in hierarchical feature extraction, making them well-suited for Neikuri images, where small but important pixel-level variations must be detected. Each CNN model offers distinct advantages tailored to processing these ambiguous images.

1) DenseNet

DenseNet introduces dense connections between layers, where each layer receives inputs from all preceding layers, allowing maximum feature reuse. This feature is particularly effective for Neikuri images, which require retaining subtle changes in image features across the network to determine the diagnostic outcome. DenseNet leverages L2 normalization and

batch normalization to maintain feature consistency, reducing the vanishing gradient problem by creating direct pathways between early and later layers. This study used the DenseNet-121 variant due to its manageable computational load and superior feature extraction capabilities. Although DenseNet proved effective at capturing intricate details, it required longer training times due to the high number of interlayer connections, resulting in extended backpropagation cycles during optimization [17].

2) ResNet

ResNet (Residual Networks) addresses the vanishing gradient problem through residual connections that allow gradients to bypass intermediate layers. This structure is particularly effective for Neikuri images, which lack clear boundaries, as it enables the model to capture detailed hierarchical representations of the oil patterns. This study employed ResNet-50, which uses bottleneck layers for dimensionality reduction before applying convolutions. This compression is advantageous in Neikuri analysis, where much of the spatial information can be redundant. The bottleneck layers help the model focus on the relevant diagnostic features. ResNet's use of 3×3 convolutions enables fine-grained feature extraction essential for the pixel-level variations seen in Neikuri images [18-22].

3) VGG-19

The architecture of VGG-19 is characterized by its simple and homogeneous design, with multiple stacked 3×3 convolutional filters and max-pooling layers. These create deep feature maps, enabling the model to capture fine details in images with complex textures, such as Neikuri oil droplets. However, the simplicity of VGG-19's design comes at the cost of a substantial memory footprint and longer inference times. The implementation of VGG-19, with approximately 144 million parameters, required significant computational resources during training and inference. This makes it less suitable for low-resource environments, although it provides a strong baseline for performance. While VGG-19 excelled at extracting dense features, it struggled with overfitting due to the limited size of the dataset, despite the inclusion of dropout regularization [23-26].

4) Inception

Inception, also known as GoogLeNet, utilizes a multiscale architecture, employing 1×1, 3×3, and 5×5 convolutions within the same layer to capture image features at various scales. This is particularly beneficial for Neikuri images, where oil droplet patterns may vary in size and distribution. This study used Inception v3, which employs factorized convolutions to reduce computational complexity. Additionally, the auxiliary classifier was activated to combat the complexity and ambiguity of the Neikuri images by improving gradient propagation through intermediate layers. However, mixed-precision training was necessary to balance computational resource usage and accuracy, given the model's high data demands. Despite these optimizations, Inception required extensive data for optimal performance, limiting its applicability to small datasets such as the one used in this study [27].

5) EfficientNet

EfficientNet employs a compound scaling method that scales depth, width, and resolution in a balanced way to achieve superior performance with fewer parameters. This model is particularly effective for Neikuri images, where efficient feature extraction is critical due to the limited dataset size. This study used the EfficientNet-B0 variant, which provided an optimal trade-off between accuracy and computational demands. A key innovation in EfficientNet is the use of Squeeze-and-Excitation (SE) blocks, which reweight channel-wise feature maps adaptively to amplify relevant features during training. This feature is especially useful in Neikuri image analysis, where subtle intensity shifts and texture differences must be emphasized. EfficientNet also incorporates swish activation functions, which improve gradient flow during training, enabling more effective learning of nuanced features [28-30].

B. Technical Suitability for Neikuri Image Analysis

The comparative analysis of these five architectures revealed that each model has unique technical strengths when applied to Neikuri images:

- DenseNet is ideal for tasks that require retaining intricate details, due to its dense feature reuse. However, it suffers from long training times due to the connected layers.
- ResNet provides deep, gradient-efficient learning, making it robust for subtle, complex feature extraction, particularly in deeper networks.
- VGG-19 offers a strong performance baseline but has high computational demands and parameter count, making it less suitable for low-resource environments.
- Inception excels at multiscale processing but requires extensive data and computational power, limiting its practical deployment for small datasets.
- EfficientNet stands out for its resource-efficient architecture, delivering high accuracy on limited datasets with fewer computational resources, making it highly applicable for real-world Neikuri analysis settings.

This study demonstrates that while performance metrics such as accuracy and loss are important, architectural nuances must also be considered when handling ambiguous medical images such as those found in Neikuri analysis. Each model's trade-offs need to be balanced depending on the deployment environment, dataset size, and hardware availability.

IV. RESULTS

The evaluation process revealed variations in performance across the different pre-trained CNN models employed during the training and testing phases. This highlights the importance of selecting the appropriate model architecture, suitable for the specific characteristics of the dataset. The ResNet architecture achieved a notable test accuracy of 88.57% on the 15-class classification task. Furthermore, most classes exhibited precision, recall, and F1-score values that exceeded 80%. These results demonstrate the model's strong capability for accurate classification within the Neikuri image dataset.

However, it is important to note that a small subset of classes yielded lower performance metrics. This observation suggests potential areas for improvement and highlights the need for further investigation. Future research efforts may focus on techniques to enhance the model's performance for these specific classes. Figure 4 shows the performance metrics of the ResNet model.

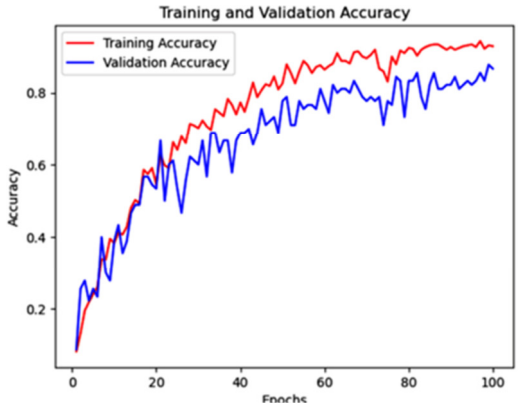

Fig. 2. Accuracy graph of the ResNet model.

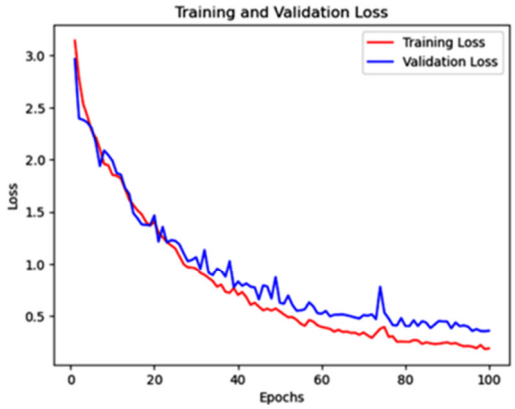

Fig. 3. Loss graph of the ResNet model.

```
Evaluation Metrics:
Test Loss: 0.3399
Test Accuracy: 0.8857
Training Time: 307.69 seconds
              precision    recall  f1-score   support

           0       0.86      0.86      0.86         7
           1       0.86      0.86      0.86         7
           2       0.00      0.00      0.00         7
           3       1.00      1.00      1.00         7
           4       0.50      1.00      0.67         7
           5       1.00      1.00      1.00         7
           6       1.00      1.00      1.00         7
           7       1.00      1.00      1.00         7
           8       1.00      0.71      0.83         7
           9       1.00      1.00      1.00         7
          10       0.75      0.86      0.80         7
          11       1.00      1.00      1.00         7
          12       1.00      1.00      1.00         7
          13       1.00      1.00      1.00         7
          14       0.88      1.00      0.93         7

    accuracy                           0.89       105
   macro avg       0.86      0.89      0.86       105
weighted avg       0.86      0.89      0.86       105
```

Fig. 4. Performance metrics of the ResNet model.

The DenseNet architecture yielded a remarkable test accuracy of 93.33% on the Neikuri image dataset, outperforming the other models. Although the model achieved excellent performance in most classes, a challenge was observed with a select few. This suggests potential avenues for targeted improvement strategies. The detailed performance measures for all classes are presented in Figures 5, 6, and 7, respectively. These figures provide a visual representation of the model's effectiveness in classifying various Neikuri image categories.

Fig. 5. Accuracy graph of the DenseNet model.

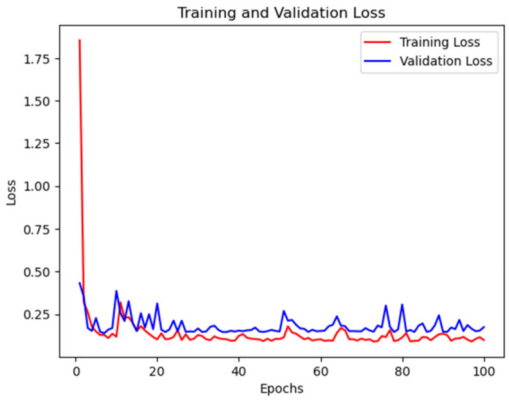

Fig. 6. Loss graph of the DenseNet model.

```
Evaluation Metrics:
Test Loss: 0.1496
Test Accuracy: 0.9333
Training Time: 362.59 seconds
              precision    recall  f1-score   support

           0       1.00      1.00      1.00         7
           1       1.00      1.00      1.00         7
           2       0.00      0.00      0.00         7
           3       1.00      1.00      1.00         7
           4       0.50      1.00      0.67         7
           5       1.00      1.00      1.00         7
           6       1.00      1.00      1.00         7
           7       1.00      1.00      1.00         7
           8       1.00      1.00      1.00         7
           9       1.00      1.00      1.00         7
          10       1.00      1.00      1.00         7
          11       1.00      1.00      1.00         7
          12       1.00      1.00      1.00         7
          13       1.00      1.00      1.00         7
          14       1.00      1.00      1.00         7

    accuracy                           0.93       105
   macro avg       0.90      0.93      0.91       105
weighted avg       0.90      0.93      0.91       105
```

Fig. 7. Performance metrics of the DenseNet model.

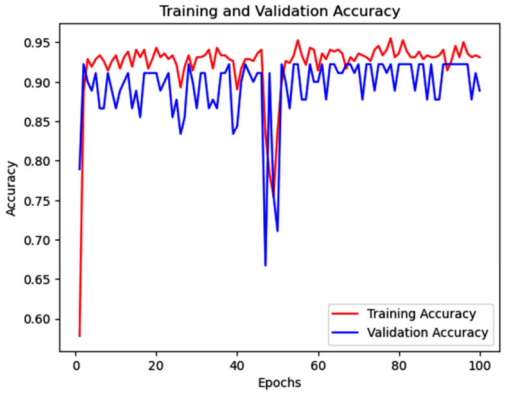

Fig. 8. Accuracy graph of the Inception v3 model.

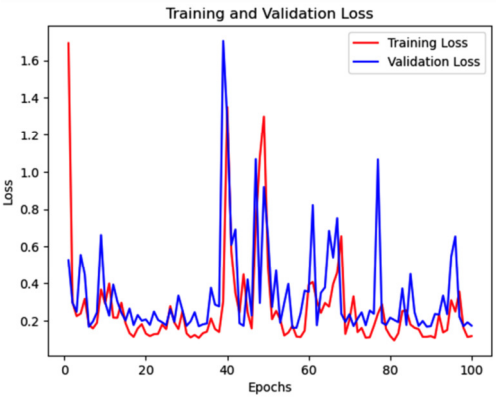

Fig. 9. Loss of the Inception v3 model.

Evaluation Metrics:
Test Loss: 0.1489
Test Accuracy: 0.9048
Training Time: 358.82 seconds

	precision	recall	f1-score	support
0	1.00	1.00	1.00	7
1	1.00	1.00	1.00	7
2	0.36	0.57	0.44	7
3	1.00	1.00	1.00	7
4	0.00	0.00	0.00	7
5	1.00	1.00	1.00	7
6	1.00	1.00	1.00	7
7	1.00	1.00	1.00	7
8	1.00	1.00	1.00	7
9	1.00	1.00	1.00	7
10	1.00	1.00	1.00	7
11	1.00	1.00	1.00	7
12	1.00	1.00	1.00	7
13	1.00	1.00	1.00	7
14	1.00	1.00	1.00	7
accuracy			0.90	105
macro avg	0.89	0.90	0.90	105
weighted avg	0.89	0.90	0.90	105

Fig. 10. Performance metrics of the Inception v3 model.

The Inception v3 model achieved an overall test accuracy of 90.5% on the Neikuri image dataset. Although achieving strong performance in most classes, the model encountered challenges in some classes. This observation suggests opportunities for targeted improvement strategies. Figures 8-10 provide a visual representation of the Inception v3 model's performance. Figure 9 shows the data loss graph, visualizing the model's learning process and convergence behavior. Figure 10 presents the performance scores for each class, including precision, recall, F1-score, and support. These metrics offer a detailed breakdown of the model's effectiveness in classifying various Neikuri image categories.

The VGG-19 model achieved an overall test accuracy of 89.5% on the Neikuri image dataset. Similar to other models, it excelled in most classes but encountered difficulties with a few, suggesting the potential for targeted improvements. Figures 11-13 depict the performance of the VGG-19 model. Figure 13 showcases the performance achieved for different classes. These visualizations aid in understanding the model's behavior and potential areas for optimization.

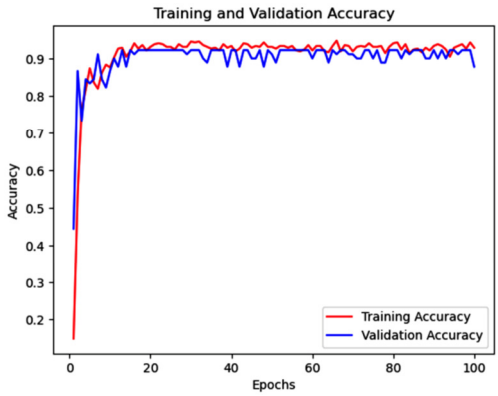

Fig. 11. Accuracy graph of the VGG-19 model.

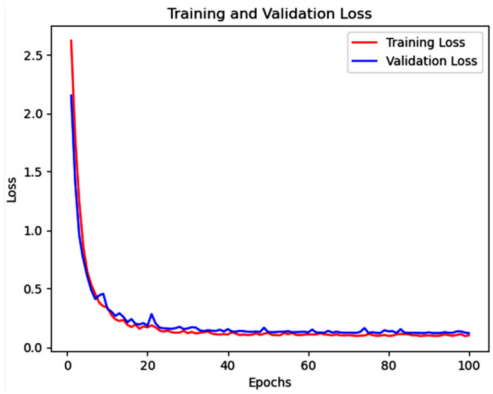

Fig. 12. Loss graph of the VGG-19 model.

Evaluation Metrics:
Test Loss: 0.1031
Test Accuracy: 0.8952
Training Time: 477.44 seconds

	precision	recall	f1-score	support
0	1.00	1.00	1.00	7
1	1.00	1.00	1.00	7
2	0.25	0.29	0.27	7
3	1.00	1.00	1.00	7
4	0.17	0.14	0.15	7
5	1.00	1.00	1.00	7
6	1.00	1.00	1.00	7
7	1.00	1.00	1.00	7
8	1.00	1.00	1.00	7
9	1.00	1.00	1.00	7
10	1.00	1.00	1.00	7
11	1.00	1.00	1.00	7
12	1.00	1.00	1.00	7
13	1.00	1.00	1.00	7
14	1.00	1.00	1.00	7
accuracy			0.90	105
macro avg	0.89	0.90	0.89	105
weighted avg	0.89	0.90	0.89	105

Fig. 13. Performance metrics of the VGG-19 model.

The EfficientNet model exhibited the lowest overall performance among the models evaluated, achieving only 6.67% accuracy. This suggests significant limitations in its ability to accurately classify Neikuri images. High data loss and low precision, recall, and F1-score metrics across most classes highlight the need for comprehensive model adjustments. A detailed breakdown of EfficientNet's performance is presented in Figures 14-16.

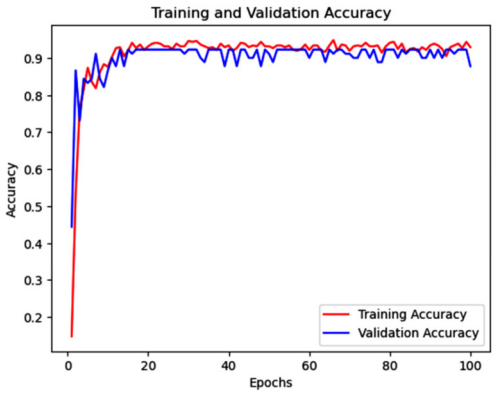

Fig. 14. Accuracy graph of EfficientNet.

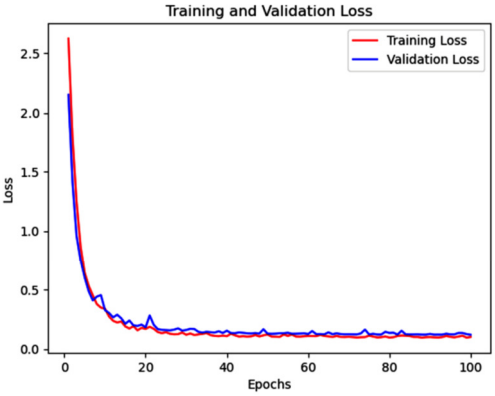

Fig. 15. Loss graph of the EfficientNet model.

```
Evaluation Metrics:
Test Loss: 2.7608
Test Accuracy: 0.0667
Training Time: 211.53 seconds
              precision    recall  f1-score   support

           0       0.00      0.00      0.00         7
           1       0.00      0.00      0.00         7
           2       0.00      0.00      0.00         7
           3       0.00      0.00      0.00         7
           4       0.00      0.00      0.00         7
           5       0.00      0.00      0.00         7
           6       0.00      0.00      0.00         7
           7       0.00      0.00      0.00         7
           8       0.00      0.00      0.00         7
           9       0.00      0.00      0.00         7
          10       0.00      0.00      0.00         7
          11       0.00      0.00      0.00         7
          12       0.00      0.00      0.00         7
          13       0.00      0.00      0.00         7
          14       0.07      1.00      0.12         7

    accuracy                           0.07       105
   macro avg       0.00      0.07      0.01       105
weighted avg       0.00      0.07      0.01       105
```

Fig. 16. Performance metrics of the EfficientNet model.

Table I presents the consolidated results of the five CNN models. This table summarizes the performance metrics, including accuracy, precision, recall, F1-score, and training time, for each model. DenseNet exhibited the highest accuracy, while EfficientNet struggled with both classification and accuracy.

TABLE I. PERFORMANCE COMPARISON OF ALL FIVE CNN MODELS

Model	Acc (%)	Precision	Recall	F1-score	Training time (s)
ResNet	88.57	High (0.86)	High (0.89)	High (0.86)	307.69
DenseNet	93.33	Excellent (0.90)	Excellent (0.93)	Excellent (0.91)	362.59
Inception v3	90.48	High (0.89)	Excellent (0.90)	Excellent (0.90)	358.82
VGG-19	89.52	High (0.89)	Excellent (0.90)	High (0.89)	477.44
EfficientNet	6.67	Very Low (0.0)	Very Low (0.07)	Very Low (0.01)	211.53

V. CONCLUSION

This study explored the efficacy of deep learning models in classifying Neikuri images, a diagnostic tool used in Siddha medicine. The results demonstrated an encouraging potential for these models in analyzing such medical imagery. However, performance varied across different models, and DenseNet achieved the highest accuracy (93.33%). Although most models exhibited strong performance in most classes, they showed limitations in classifying specific categories. This observation highlights the need for further research to refine these models and address these class-specific weaknesses. In particular, EfficientNet exhibited significantly lower accuracy (6.67%), suggesting a requirement for a more tailored approach to this particular architecture. Overall, the findings support the continued exploration of deep learning for Neikuri image analysis in Siddha medicine. Future efforts should focus on optimizing models to address identified weaknesses and develop a reliable tool for accurate Neikuri image classification.

ACKNOWLEDGMENTS

This research endeavor would not have been possible without the invaluable contributions of the Siddha medical practitioners who provided their expertise and guidance. The authors express their sincere gratitude to the exceptional team at the Government College of Siddha, Arumbakkam, Chennai, India, whose unwavering support and dedication to their practice were instrumental throughout this research journey. Their partnership was crucial to the success of this project. The authors also express deep appreciation to Alliance University, Bangalore, India, for its continuous support throughout the research process.

REFERENCES

[1] A. B. Abdul Bari, P. J. Samuel, M. D. Chandrasekar, R. Shyamala, and S. S. Rangasamy, "Towards Standardization–A New Protocol for Oil drop test (Neikuri) in Healthy Subjects," *International Journal of Pharmacology and Clinical Sciences*, vol. 4, no. 4, pp. 83–89, Feb. 2016, https://doi.org/10.5530/ijpcs.4.4.3.

[2] K. B. Kachare and A. C. Kar, "Important aspect of Ayurvedic taila bindu pariksha to assesses disease prognosis," *World Journal of Pharmaceutical Research*, vol. 4, no. 2, pp. 851–860, Dec. 2014.

[3] J. Jeyavenkatesh, S. R. Ramani, P. Saravanapandian, P. M. Bai, and R. S. Priya, "An Observational Cross-sectional Single Arm Trial and Perspective Study of Siddha Diagnostic Tool Neerkuri and Neikuri (Uroscopy) in COVID-19 Patients," *Journal of Complementary and Alternative Medical Research*, pp. 51–58, Sep. 2022, https://doi.org/10.9734/jocamr/2022/v19i130369.

[4] G. Dhinesh Raman, "A Study on Documentation of Siddha Diagnostic Methods Specially Naadi, Neerkuri and Neikuri for Praana Vaadha Kurigal," Ph.D. dissertation, Government Siddha Medical College, Palayamkottai, India, 2019.

[5] K. R. V. Darshini, "Comparative study of the Siddha Diagnostic Methods Specially Neerkuri & Neikuri with Modern Diagnostic Methods in Neerizhivu Madhumeham (Diabetes Mellitus–Type 2)," Ph.D. dissertation, Government Siddha Medical College, Palayamkottai, India, 2018.

[6] V. Rohini, "A Study on Siddha Diagnostic Methodology of Neerkuri and Neikuri for" SOMA ROGAM"," Ph.D. dissertation, Government Siddha Medical College, Palayamkottai, India, 2022.

[7] V. Dhivya, "A Clinical study on Documentation of Thaehiyin Ilakkanam compared with Neikuri in Siddha Science and Blood Grouping in Modern Science," Ph.D. dissertation, Government Siddha Medical College, Palayamkottai, India, 2019.

[8] M. Wolfgram, "Truth Claims and Disputes in Ayurveda Medical Science," *Journal of Linguistic Anthropology*, vol. 20, no. 1, pp. 149–165, Jun. 2010, https://doi.org/10.1111/j.1548-1395.2010.01054.x.

[9] R. Meena *et al.*, "Fluorescent carbon dots driven from ayurvedic medicinal plants for cancer cell imaging and phototherapy," *Heliyon*, vol. 5, no. 9, Sep. 2019, Art. no. e02483, https://doi.org/10.1016/j.heliyon.2019.e02483.

[10] A. Mukherjee, M. Banerjee, V. Mandal, A. C. Shukla, and S. C. Mandal, "Modernization of Ayurveda: A Brief Overview of Indian Initiatives," *Natural Product Communications*, vol. 9, no. 2, Feb. 2014, Art. no. 1934578X1400900239, https://doi.org/10.1177/1934578X1400900239.

[11] V. Patil and U. K. Sapra, "Clinical Diagnosis in Ayurveda: Concepts, Currnt Practice and Prospects," *Journal of Ayurveda and Holistic Medicine (JAHM)*, vol. 1, no. 2, Apr. 2021, https://doi.org/10.70066/jahm.v1i2.420.

[12] S. Chen, Z. Sedghi Gamechi, F. Dubost, G. Van Tulder, and M. De Bruijne, "An end-to-end approach to segmentation in medical images with CNN and posterior-CRF," *Medical Image Analysis*, vol. 76, Feb. 2022, Art. no. 102311, https://doi.org/10.1016/j.media.2021.102311.

[13] S. Atasever, N. Azginoglu, D. S. Terzi, and R. Terzi, "A comprehensive survey of deep learning research on medical image analysis with focus on transfer learning," *Clinical Imaging*, vol. 94, pp. 18–41, Feb. 2023, https://doi.org/10.1016/j.clinimag.2022.11.003.

[14] G. Litjens *et al.*, "A survey on deep learning in medical image analysis," *Medical Image Analysis*, vol. 42, pp. 60–88, Dec. 2017, https://doi.org/10.1016/j.media.2017.07.005.

[15] S. Suganyadevi, V. Seethalakshmi, and K. Balasamy, "A review on deep learning in medical image analysis," *International Journal of Multimedia Information Retrieval*, vol. 11, no. 1, pp. 19–38, Mar. 2022, https://doi.org/10.1007/s13735-021-00218-1.

[16] H. P. Chan, R. K. Samala, L. M. Hadjiiski, and C. Zhou, "Deep Learning in Medical Image Analysis," in *Deep Learning in Medical Image Analysis : Challenges and Applications*, G. Lee and H. Fujita, Eds. Cham, Switzerland: Springer International Publishing, 2020, pp. 3–21.

[17] A. S. Parihar and A. Java, "Densely connected convolutional transformer for single image dehazing," *Journal of Visual Communication and Image Representation*, vol. 90, Feb. 2023, Art. no. 103722, https://doi.org/10.1016/j.jvcir.2022.103722.

[18] A. Jaiswal, Deepali, and N. Sachdeva, "Empirical Analysis of Traffic Sign Recognition using ResNet Architectures," in *2023 3rd International Conference on Advance Computing and Innovative Technologies in Engineering (ICACITE)*, Greater Noida, India, May 2023, pp. 280–285, https://doi.org/10.1109/ICACITE57410.2023.10183247.

[19] G. Kılıçarslan, C. Koç, F. Özyurt, and Y. Gül, "Breast lesion classification using features fusion and selection of ensemble ResNet method," *International Journal of Imaging Systems and Technology*, vol. 33, no. 5, pp. 1779–1795, 2023, https://doi.org/10.1002/ima.22894.

[20] R. K.P. and S. V., "Machine Learning Approach for Mixed type Wafer Defect Pattern Recognition by ResNet Architecture," in *2023 International Conference on Control, Communication and Computing (ICCC)*, Thiruvananthapuram, India, May 2023, pp. 1–6, https://doi.org/10.1109/ICCC57789.2023.10165078.

[21] N. Shahadat and A. S. Maida, "Enhancing ResNet Image Classification Performance by Using Parameterized Hypercomplex Multiplication," in *2023 26th International Conference on Computer and Information Technology (ICCIT)*, Cox's Bazar, Bangladesh, Dec. 2023, pp. 1–6, https://doi.org/10.1109/ICCIT60459.2023.10441211.

[22] S. Showkat and S. Qureshi, "Efficacy of Transfer Learning-based ResNet models in Chest X-ray image classification for detecting COVID-19 Pneumonia," *Chemometrics and Intelligent Laboratory Systems*, vol. 224, May 2022, Art. no. 104534, https://doi.org/10.1016/j.chemolab.2022.104534.

[23] R. Mohan, K. Ganapathy, A. Rama, "Brain tumour classification of Magnetic resonance images using a novel CNN based Medical Image Analysis and Detection network in comparison with VGG16," *Journal of Population Therapeutics and Clinical Pharmacology*, vol. 28, no. 2, Jan. 2022, https://doi.org/10.47750/jptcp.2022.873.

[24] Z. Cao, J. Huang, X. He, and Z. Zong, "BND-VGG-19: A deep learning algorithm for COVID-19 identification utilizing X-ray images," *Knowledge-Based Systems*, vol. 258, Dec. 2022, Art. no. 110040, https://doi.org/10.1016/j.knosys.2022.110040.

[25] Z. Hu, Z. Wang, Y. Jin, and W. Hou, "VGG-TSwinformer: Transformer-based deep learning model for early Alzheimer's disease prediction," *Computer Methods and Programs in Biomedicine*, vol. 229, Feb. 2023, Art. no. 107291, https://doi.org/10.1016/j.cmpb.2022.107291.

[26] S. Anwar, S. R. Soomro, S. K. Baloch, A. A. Patoli, and A. R. Kolachi, "Performance Analysis of Deep Transfer Learning Models for the Automated Detection of Cotton Plant Diseases," *Engineering, Technology & Applied Science Research*, vol. 13, no. 5, pp. 11561–11567, Oct. 2023, https://doi.org/10.48084/etasr.6187.

[27] Z. Li, L. Zhang, Z. Zhang, R. Xu, and D. Zhang, "Speckle classification of a multimode fiber based on Inception V3," *Applied Optics*, vol. 61, no. 29, pp. 8850–8858, Oct. 2022, https://doi.org/10.1364/AO.463764.

[28] V. Ravi and R. Chaganti, "EfficientNet deep learning meta-classifier approach for image-based android malware detection," *Multimedia Tools and Applications*, vol. 82, no. 16, pp. 24891–24917, Jul. 2023, https://doi.org/10.1007/s11042-022-14236-6.

[29] X. Chen *et al.*, "Application of EfficientNet-B0 and GRU-based deep learning on classifying the colposcopy diagnosis of precancerous cervical lesions," *Cancer Medicine*, vol. 12, no. 7, pp. 8690–8699, 2023, https://doi.org/10.1002/cam4.5581.

[30] A. Abdelrahman and S. Viriri, "EfficientNet family U-Net models for deep learning semantic segmentation of kidney tumors on CT images," *Frontiers in Computer Science*, vol. 5, Sep. 2023, https://doi.org/10.3389/fcomp.2023.1235622.